Received: March 9, 2025 | Revised: June 23, 2025 | Accepted: June 25, 2025

JOURNAL OF APPLIED RESEARCH ON SCIENCE AND TECHNOLOGY
JARST
INSTITUTE OF RESEARCH AND DEVELOPMENT
RAJAMANGALA UNIVERSITY OF TECHNOLOGY THANYABURI
ISSN ONLINE: 2773-9473
https://ph01.tci-thaijo.org/index.php/rmutt-journal

Prediction of the fatigue life of elevator wire rope using the Grey model GM (1,1)

Sittiphan Subcharoen, Pipat Pramot, Terdkiat Limpeteeprakarn, Apisit Muanmuang and Manusak Janthong*
Department of Mechanical Engineering, Faculty of Engineering, Rajamangala University of Technology Thanyaburi, Pathum Thani 12120, THAILAND
*Corresponding author: manusak.j@en.rmutt.ac.th

ABSTRACT

This article presents a tensile testing method for elevator wire ropes to predict fatigue life using the Grey GM (1,1) model, based on the relationship between applied force and the service life of the wire rope. The model is constructed from testing data where forces are applied to the wire rope until failure or damage occurs. A tensile testing machine for elevator wire ropes was designed and constructed, with a 5-meter-tall steel frame structure. At the top, a driving machine consisting of a 7.5-horsepower motor was installed to pull a wire rope with a diameter of 10 millimeters. One end of the wire rope is attached to the lift car, while the other is connected to the counterweight, enabling two-level vertical movement. The tensile force simulation involved adding masses of 350, 450, 550, and 650 kilograms, which moved up and down and stopped abruptly. The peak tensile forces recorded in the wire rope were 3.641, 4.845, 6.666, and 7.873 kilonewtons, respectively. The predicted fatigue life of the wire rope corresponding to these forces was 1,347,302; 927,853; 638,988; and 440,055 cycles. The results show that the fatigue life of the wire rope decreases as the tensile force increases. Predicting the fatigue life of wire ropes is crucial for inspection and quality assessment of elevator ropes. It allows for estimating wear over time in accordance with the Ministerial Regulation on Standards for Safety Management, Occupational Health, and Working Environment concerning Machinery, Cranes, and Boilers B.E. 2564 (2021).

Keywords: Wire rope, Predict the fatigue life, Wear and tear over time

INTRODUCTION

Wire ropes are essential equipment used for lifting or pulling heavy loads in various industrial applications, such as bridges, elevators, and mining hoists [1-3]. During operation, friction and wear issues arise due to differing contact conditions of the wire rope [4, 5], leading to changes in its properties. Damage may occur due to mechanical or environmental factors, or a combination of both [6, 7], which reduces performance and causes fractures [8, 9]. The complexity of wire rope wear accelerates its degradation [10].

Furthermore, deteriorating wire ropes exhibit increased elasticity, resulting in system vibrations during operation [11], posing safety hazards to users and workers [12]. Therefore, the efficiency and safety of the wire rope are critically important. Ensuring reliable elevator operation necessitates adherence to safety standards [13-15] relevant to wire rope usage. These standards cover requirements for design, testing, installation, and maintenance [16, 17], ensuring that wire ropes perform efficiently and safely.

For wire rope analysis techniques, Anil et al. [18] analyzed elevator wire rope using the Ansys program to identify best practices for managing wire rope to enhance safety and minimize elevator downtime due to rope failures. Yuanpei et al. [19] developed a finite element model of wire rope to study mechanical properties such as stress and strain, contributing to wire rope wear.

Bassir et al. [20] investigated the effects of corrosion on wire rope by immersing it in sulfuric acid and subjecting it to static traction tests to predict lifespan for maintenance planning. Yuxing [21] examined the friction and wear characteristics of fiber core wire rope (6x19+FC structure) under low-temperature environments, finding that the friction coefficient increased as ambient temperature decreased, peaking at 0.85 at -25°C, which could be mitigated by oil lubrication.

Zhen et al. [22] explored tribo-fatigue behavior by conducting bending fatigue tests on wire rope. Their study revealed that the rope's diameter decreased as bending fatigue increased, leading to damage and fractures. Xiangdong et al, [23] analyzed the sliding friction coefficient (COF), discovering that wire rope surface wear exhibited distinct patterns, including delamination, deep grooves, and plastic deformation. These effects were

DOI: 10.60101/jarst.2024.260813

significantly influenced by sliding speed, which also impacted the contact area of wire rope strands [24].

This study presents a tensile test of elevator wire rope to predict the forces acting within the wire rope. A Grey GM (1,1) model was developed to identify the relationship between force and the lifespan of the wire rope. This model aims to predict fatigue life from usage, which is crucial for inspecting and assessing the quality of elevator wire rope to ensure that elevators operate safely and efficiently.

MATERIALS AND METHODS

1. Structural design

The elevator wire rope tensile test machine's structural design consists of a steel framework, with a height of 5 meters. At the top, an elevator machine (driving machine) is installed, which includes a 7.5 horsepower motor used to pull the wire rope with a diameter of 10 millimeters. The ends of the wire rope are attached to both the lift car and the counterweight assembly, which moves up and down. There are two levels: the first level is 0.6 meters above the ground, the second level is 1.7 meters above the first, and the distance from the second level to the motor mount is 1 meter, as shown in Figure 1.

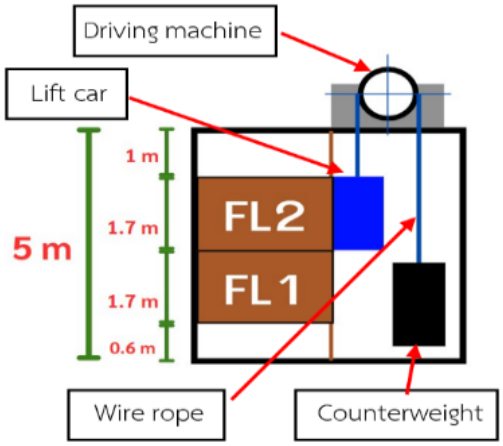

Figure 1 Structural design for testing the strength in the lift sling cable.

2. Control system

The design of the control system for the lift sling cable tensile testing machine is divided into two parts: the power circuit and the control circuit.

2.1 The power circuit consists of a fuse, which protects against short circuits and excessive current in the electrical circuit, connected to a magnetic contactor. A magnetic contactor is an electrical device that opens or closes an electrical circuit through magnetic control. It is used to control the operation of an electric motor. The motor used is an AC three-phase motor, which has advantages such as no brushes, resulting in low friction loss, high power factor, low maintenance, easy startup, relatively constant speed, ease of construction, durability, low cost, and high efficiency, as shown in Figure 2.

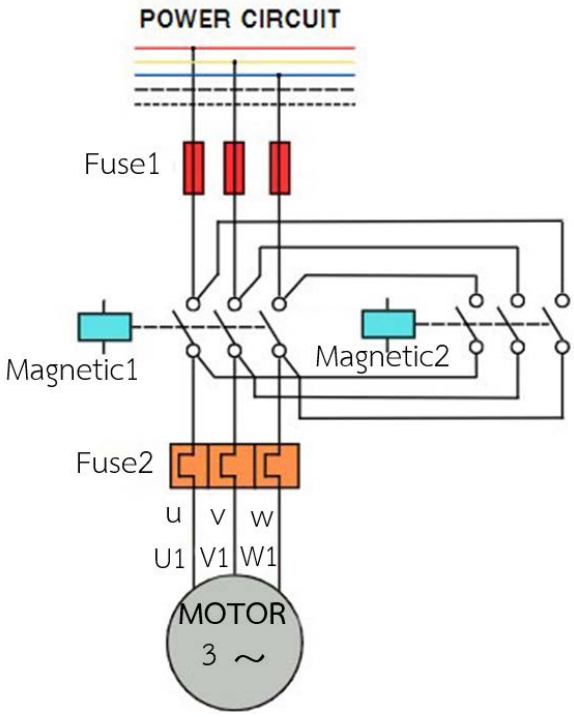

Figure 2 Motor power circuit.

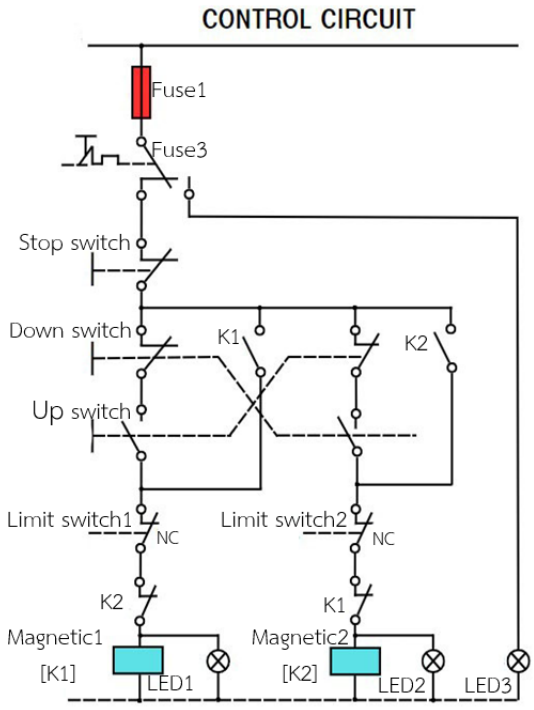

Figure 3 Motor Control Circuit.

2.2 The control circuit consists of a fuse that is connected to an overload relay (Overload Relay) to disconnect the control circuit. This is a protective device to prevent electrical equipment from exceeding its capacity or to protect the motor from damage when the current exceeds the rated load

DOI: 10.60101/jarst.2024.260813

capacity. It includes switches that command the lift to move in two directions: the up switch and the down switch. The movement will stop automatically due to the limit switches installed on each floor. However, in the event of an abnormality, a Stop switch will halt the operation for safety. The status of the operation is indicated by signal lights as shown in Figure 3.

3. Design of measurement systems

3.1 Circuit design measurement Strain refers to an object's deformation amount compared to its original size. It is a fundamental principle used to measure the strength of various materials, including checking the strength of the lift's wire rope. This ensures the safety and reliability of the lift system. A strain gauge measures the elongation or contraction of the lift's wire rope. It is attached to a metal bar placed between the wire rope and the lift cabin, as shown in Figure 4. When the motor pulls the wire rope, it causes strain on the metal bar, leading to a change in its shape, which also results in a change in the resistance of the strain gauge.

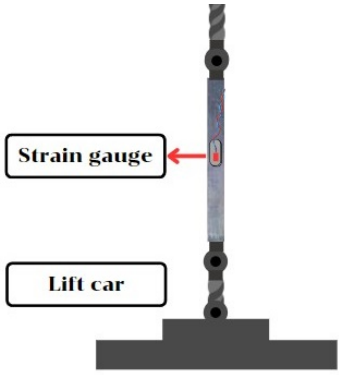

Figure 4 Attaching the strain gauge to the metal bar.

Test

Test No.	Area mm²	Max. Load kN	Tensile strength N/ mm²	Yield point kN	Yield strength N/ mm²
1	81.00	38.71	477.95	26.18	323.21
2	122.72	63.55	571.85	63.24	515.36

Figure 5 Results of the tensile test on a steel bar.

A metal bar is used instead of a wire rope, since installing a strain gauge requires a smooth surface for accurate strain measurements, and the surface of a wire rope is not smooth, a metal bar is used instead. The metal bar must have properties that closely resemble the wire rope. The bar used has been tested for tensile strength, which is 477.95 Newtons per square millimeter, as shown in Figure 5. The wire rope used is a right-hand ordinary lay type with an 8×S (19) + FC construction, as shown in Figure 6. The tensile strength of the wire rope is 482.92 Newtons per square millimeter, as shown in Figure 7.

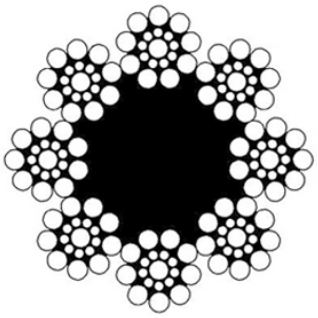

Figure 6 Helical characteristics of 8×S (19) + FC wire rope [25].

Test date : 10 February 2023

Test Temperature : 25 ℃

Testing machine : Universal Testing Machine INSTRON 5590-HVL

Table 1 the results of tensile test of SLING Size 10.45 mm

Specimen	T
Diameter (mm)	10.45
Cross sectional area (mm^2)	85.77
Maximum tensile load (kN)	41.42
Tensile strength (N/mm^2)	482.92

Figure 7 Results of the wire rope tensile test for Thailand Institute of Scientific and Technological Research (TISTR) Request No. R6600254.

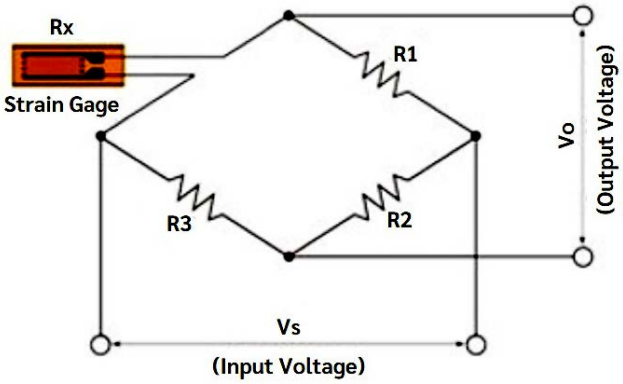

Figue 8 ¼ Wheatstone bridge circuit [26].

Measuring values from the strain gauge, to measure the values obtained from a strain gauge, a wheatstone bridge circuit is used [26] This circuit is designed to determine unknown resistance values by comparing them with standard known resistances. It is particularly effective in converting small changes in electrical resistance, as detected by the strain gauge, into an output voltage. The process involves supplying input voltage (referred to as excitation) to the circuit. The output voltage is then measured based on changes in resistance within the circuit. These changes are caused by the strain gauge's response to deformation. The resulting output is expressed in units of mV/V, as illustrated in Figure 8.

From Figure 8 the governing equation [27] can be derived as follows;

DOI: 10.60101/jarst.2024.260813

JOURNAL OF APPLIED RESEARCH ON SCIENCE AND TECHNOLOGY

$$V_0 = (\frac{R_3}{R_1+R_3} - \frac{R_x}{R_2+R_x})V_S \quad (1)$$

By determining the stress value from the resistance relationship when specified. $R_x = F\varepsilon$ [28].

$$\varepsilon = \frac{4V_0}{V_{in}*A*F} \quad (2)$$

When R_1 is Resistor 1

R_2 is Resistor 2

R_3 is Resistor 3

R_x is Strain gauge signal

ε is Strain

V_0 is Output voltage

V_S is Input voltage

F is Gauge factor

A is Strain gauge circuit amplifier gain

3.2 Specifications

The strain gauge used is the KFGS-5-120-C1-11 L1M2R model, which functions by changing the electrical resistance that occurs when the material to which the strain gauge is attached is stretched or compressed. As the metal stretches or contracts, the electrical resistance changes accordingly. This change in resistance can be converted into strain values using a Wheatstone bridge circuit, which has the following characteristics.

- Electrical resistance
- Gauge factor
- Input voltage
- Amplification rate of the strain gauge signal amplifier

3.3 Measurement system

The Wheatstone bridge circuit designed from Figure 8 is connected to the JY-S60 amplifier, which amplifies the signal as an analog signal. This signal is then sent to the NI myRIO for processing and recording results on a notebook computer, as shown in Figure 9.

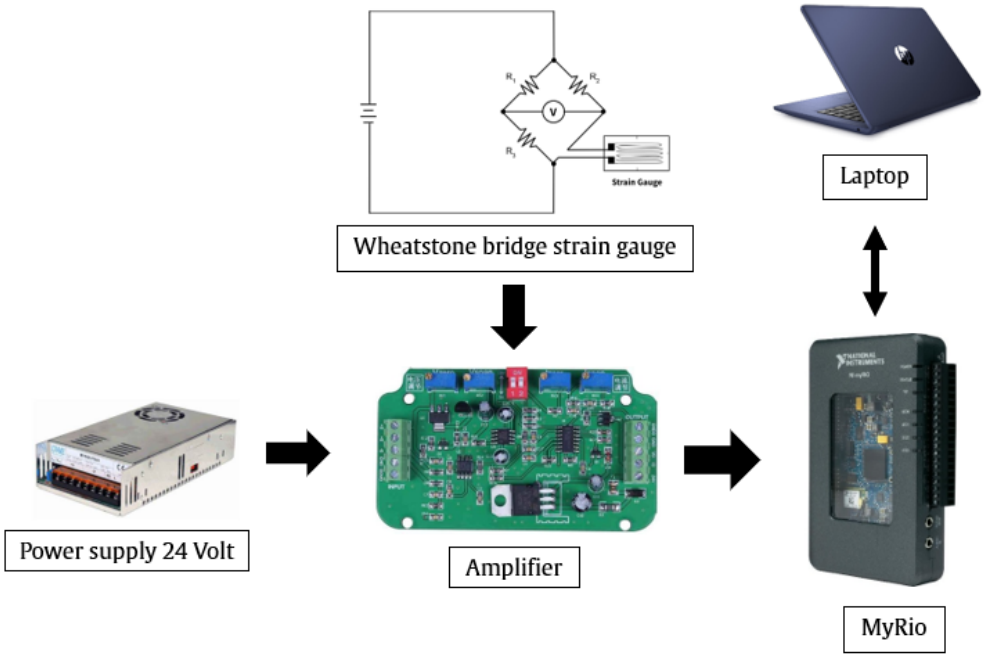

Figure 9 Measurement system equipment.

To ensure accurate prediction analysis, it is necessary to calibrate the strain gauge by applying masses of 300, 400, 500, and 600 kilograms to the lift car, which has a mass of 50 kilograms, as shown in Figure 10. The strain gauge readings in the form of voltage signals are presented in Table 1.

The values from Table 1 are plotted in a graph, as shown in Figure 11.

From Figure 11 a linear equation can be derived, which consists of the slope of the graph multiplied by the measured value, plus a constant. This linear equation should be implemented as a function in LabVIEW to convert the voltage readings into weight measurements.

3.4 The wire rope material used for securing and lifting.

The wire rope used for securing and lifting measurement equipment complies with the standards and requirements of ISO 4344 for passenger elevator applications. It meets the specified safety requirements and experimental conditions to simulate real operational scenarios. A pulley with a 10-millimeter groove diameter is used to securely hold the wire rope, ensuring firm adhesion and preventing slippage during sudden stops, as shown in Figure 12.

DOI: 10.60101/jarst.2024.260813

JOURNAL OF APPLIED RESEARCH ON SCIENCE AND TECHNOLOGY

(a)

(b)

(c)

(d)

Figure 10 Calibration of the strain gauge with added mass in the lift car 300 kg (a), 400 kg (b), 500 kg (c), and 600 kg (d).

Table 1 Strain gauge calibration.

Voltage (Volts)	Mass (kilograms)			
	350	450	550	650
	1.406	1.660	2.095	2.354
	1.416	1.694	2.031	2.334
	1.440	1.694	2.065	2.295
Average	**1.421**	**1.683**	**2.064**	**2.328**

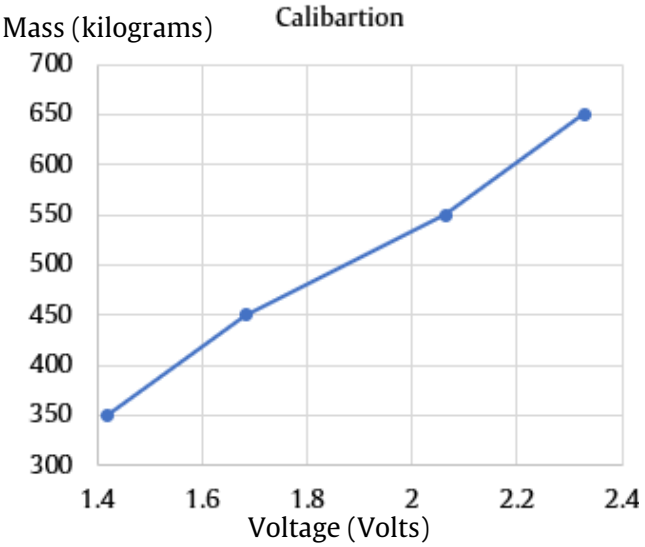

Figure 11 Strain gauge calibration.

Figure 12 Installation characteristics of the strain gauge, steel rod, and wire rope.

3.5 Testing method

In the test, the movement of the elevator will be controlled to oscillate vertically the same number of times, with a sudden stop at each instance. This is done to determine the maximum force exerted on the wire rope by measuring the strain on the material. A constant weight is added as a load applied during

DOI: 10.60101/jarst.2024.260813

JOURNAL OF APPLIED RESEARCH ON SCIENCE AND TECHNOLOGY

testing. During the sudden stop, the elevator car carrying the weight will be halted at the midpoint of the elevator shaft to induce tension or shock force on the wire rope.

RESULTS AND DISCUSSION

1. Gray GM model (1.1) The Grey Model can process complex geometric structures, mechanical models, and external conditions that affect the fatigue lifespan of wire ropes. It helps reduce the difficulty in calculating reliable predictions of the wire rope's lifespan [29-32]. The traditional form of the GM (1,1) equation is defined as follows.

$$x^{(0)}(k) + az^{(1)}(k) = b \tag{3}$$

Where $x^{(0)}(k)$ is the initial sequence, $x^{(1)}(k)$ is the first accumulated sequence, a is the developing coefficient, b is the gray action quantity , and $z^{(1)}(k)$ is the background value. This is achieved using the sequence of average values and calculating the derivative of the data sequence.

The values of a and b can be obtained using the least squares method for the GM (1,1) model as follows.

$$\begin{bmatrix} a \\ b \end{bmatrix} = (B^T B)^{-1} B^{TY} \tag{4}$$

When

$$Y = \begin{bmatrix} x^{(0)}(2) \\ x^{(0)}(3) \\ \vdots \\ x^{(0)}(n) \end{bmatrix}, \mathrm{B} = \begin{bmatrix} -z^{(1)}(2) & 1 \\ -z^{(1)}(3) & 1 \\ \vdots & \vdots \\ -z^{(1)}(3) & 1 \end{bmatrix} \tag{5}$$

The calculation of the background value is fundamentally the area enclosed by the curve of the approximation and the axes, approximated using trapezoidal areas $x^{(1)}(t)$ along the x-axis $[k-1, k]$ and the y-axis t. Due to significant errors in this method, improvements have been made, and equation (5) is referred to as the whitenization equation. It can be rewritten as follows.

$$\int_{k-1}^{k} \frac{dx^{(1)}(k)}{dt} dt + a \int_{k-1}^{k} x^{(1)}(t) dt$$

$$= b \int_{k-1}^{k} (x^{(1)}(t))^{(2)} \, dt \tag{6}$$

By rearranging the equation it can be expressed as follows.

$$x^{(0)}(k) + a \int_{k-1}^{k} x^{(1)}(t) dt$$

$$= b \int_{k-1}^{k} (x^{(1)}(t))^{(2)} \, dt \tag{7}$$

Thus, the calculation $z^{(1)}(k)$ by solving the integral, the accuracy can be enhanced. $\int_{k-1}^{k} x^{(1)}(t) dt$ can enhance the accuracy of the background value estimation. This, in turn, improves the precision of predicting the fatigue life of the wire rope using the Grey Model GM (1,1). The Newton-Cotes formula is applied to compute the integral.

$$C = \frac{b-a}{90}[7f(x_0) + 32f(x_1) + 12f(x_2) + \ldots$$

$$\ldots + 32f(x_3) + 7f(x_4)] \tag{8}$$

When $x_k = a + kh, h = (b-a)/4, a = k-1, b = k$ is applied, the background value is given by.

$$z^{(1)}(k) = C = \frac{b-a}{90}[7f(x_0) + 32f(x_1) + \ldots$$

$$\ldots + 12f(x_2) + 32f(x_3) + 7f(x_4)] \tag{9}$$

The process of predicting the fatigue life of wire ropes under tensile force is arranged in ascending order. The GM (1,1) gray model is constructed based on the original sample age data of the wire rope from Table 2, which was obtained from testing the forces affecting the wire rope's usage. The values of a and b are determined to predict the next fatigue life.

Table 2 Experimental results on the service life of wire ropes from fatigue testing machine [33].

Tension load (kN)	N_A (cycle)
S = 15	57702
S = 20	34986
S = 25	32608
S = 30	25672

2. Experimental Results in this study a simulation of the tensile load on elevator wire ropes was conducted by increasing the mass to 350, 450, 550, and 650 kilograms, allowing vertical movement up and down and then stopping abruptly to record the maximum force exerted on the wire rope as shown in Table 3. The obtained force values were then used to predict the fatigue life of the wire rope using the Grey Model GM (1,1). The results indicate that as the tensile force applied to the wire rope increases, its fatigue life decreases accordingly. For example, when the tensile force values were 3.641, 4.845, 6.666, 7.873, 9.00, 10.00, and 15.00 kN, the predicted fatigue life cycles of the wire rope were 1,347,302, 927,853, 638,988, 440,055, 303,054,

DOI: 10.60101/jarst.2024.260813

208,689, and 143,740, respectively, as shown in Figure 13 and summarized in Table 4.

Table 3 Testing of maximum force generated from weight in each experiment.

Mass (kg)	Force Testing from Weight (N)				
	1	2	3	4	Average
350	3,503	3,639	3,693	3,729	3,641
450	4,879	4,744	4,924	4,834	4,845
550	6,706	6,796	6,503	6,661	6,666
650	8,059	7,833	7,856	7,743	7,873

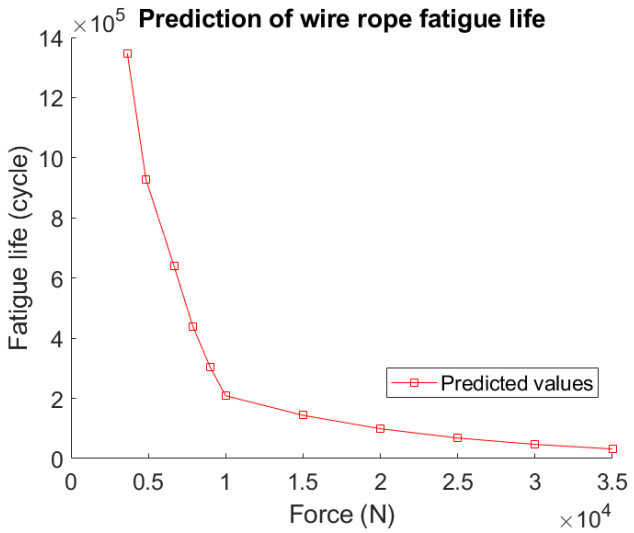

Figure 13 Prediction of wire rope fatigue life.

Table 4 Predicted Fatigue Life of Wire Rope under Tensile Load.

Tension (kN)	Fatigue life (cycle)
3.641	1,347,302
4.845	927,853
6.666	638,988
7.873	440,055
9.00	303,054
10.00	208,689
15.00	143,740

CONCLUSIONS

This research simulates the tensile load on elevator wire ropes by increasing the weight, moving up and down, and then stopping suddenly to determine the maximum force exerted on the wire rope during operation. The obtained data is used to predict the fatigue life of the wire rope. The study indicates that as the force applied to the wire rope increases, its fatigue life decreases [34-36]. Repeated tensile loading over a long period causes deterioration of the wire rope, requiring more frequent replacements. When the wire rope reaches its lifespan limit, it may lead to damage [37-39]. From tensile tests with forces of 3.641, 4.845, 6.666, 7.873, 9.00, 10.00, and 15.00 kilonewtons, the corresponding fatigue lives of the wire rope were found to be 1,347,302; 927,853; 638,988; 440,055; 303,054; 208,689; and 143,740 cycles, respectively. It is essential to predict the lifespan of the wire rope in advance for maintenance planning. the wire rope is lifespan for maintenance planning or selecting an appropriate wire rope size. These measures must comply with the Ministerial Regulation on Safety Management, Occupational Health, and Working Environment for Machinery, Cranes, and Boilers, B.E. 2564 (2021) [40], as well as other relevant standards [41-43].

ACKNOWLEDGEMENT

This research was funded by the Science, Research, and Innovation Promotion Fund for the year 2021, Office of the Commission on Science, Research, and Innovation Promotion (SIP). The grant number is FR645E0703C.4.

REFERENCES

1. Pal U, Mukhopadhyay G, Sharma A, Bhattacharya S. Failure analysis of wire rope of ladle crane in steel making shop. Int J Fatigue [Internet]. 2018; 116:149-55. Available from: http://dx.doi.org/10.1016/j.ijfatigue.2018.06.019.
2. Cao X, Wu W. The establishment of a mechanics model of multi-strand wire rope subjected to bending load with finite element simulation and experimental verification. Int J Mech Sci [Internet]. 2018;142-143:289-303. Available from: http://dx.doi.org/10.1016/j.ijmecsci.2018.04.051.
3. Wang XY, Meng XB, Wang JX, Sun YH, Gao K. Mathematical modeling and geometric analysis for wire rope strands. Appl Math Model [Internet]. 2015;39(3-4):1019-32. Available from: http://dx.doi.org/10.1016/j.apm.2014.07.015.
4. Zhang D, Feng C, Chen K, Wang D, Ni X. Effect of broken wire on bending fatigue characteristics of wire ropes. Int J Fatigue [Internet]. 2017;103: 456-65. Available from: http://dx.doi.org/10.1016/j.ijfatigue.2017.06.024.
5. Wahid A, Mouhib N, Ouardi A, Sabah F, Chakir H, ELghorba M. Experimental prediction of wire rope damage by energy method. Eng Struct [Internet]. 2019;201(109794):109794. Available from: http://dx.doi.org/10.1016/j.engstruct.2019.109794.
6. Chang XD, Huang HB, Peng YX, Li SX. Friction, wear and residual strength properties of steel

DOI: 10.60101/jarst.2024.260813

wire rope with different corrosion types. Wear [Internet]. 2020;458-9(203425):203425. Available from: http://dx.doi.org/10.1016/j.wear.2020.203425.

7. Battini D, Solazzi L, Lezzi AM, Clerici F, Donzella G. Prediction of steel wire rope fatigue life based on thermal measurements. Int J Mech Sci [Internet]. 2020;182(105761):105761. Available from: http://dx.doi.org/10.1016/j.ijmecsci.2020.105761.

8. Shu Q, Wang K, Yuan G, Zhang Y, Lu L, Liu Z. Assessing capacity of corroded angle members in steel structures based on experiment and simulation. Constr Build Mater [Internet]. 2020;244(118210):118210. Available from: http://dx.doi.org/10.1016/j.conbuildmat.2020.118210.

9. Li G, Hou C, Shen L, Yao GH. Performance and strength calculation of CFST columns with localized pitting corrosion damage. J Constr Steel Res [Internet]. 2022;188(107011):107011. Available from: http://dx.doi.org/10.1016/j.jcsr.2021.107011.

10. Xiang-dong C, Yu-xing P, Zhen-cai Z, Sheng-yong Z, Xian-sheng G, Chun-ming X. Effect of wear scar characteristics on the bearing capacity and fracture failure behavior of winding hoist wire rope. Tribol Int [Internet]. 2019;130:270-83. Available from: http://dx.doi.org/10.1016/j.triboint.2018.09.023.

11. Wu S, He P, Gong X. Analysis of transverse vibration of wire rope in flexible hoisting system. J Vibroengineering [Internet]. 2021;23(2):283-97. Available from: http://dx.doi.org/10.21595/jve.2020.21487.

12. Ray A, Dhua SK, Mishra KB, Jha S. Microstructural manifestations of fractured Z-profile steel wires on the outer layer of a failed locked coil wire rope. Pr Fail Anal [Internet]. 2003;3(4):51-5. Available from: http://dx.doi.org/10.1007/bf02715933.

13. Steel wire ropes for lifts - Minimum requirements: ISO 4344:2004(E). Geneva, Switzerland, 2004. Safety rules for the construction and installation of lifts-Part 1: Electric lifts. London: BSI Group; 2009.

14. Inspection Standard of Elevator, escalator and Dumbwaiter JIS A 4302-1992. Japan: Japanese Industrial Standard; 1992.

15. Thangavel D. Study of occupational health and safety: Elevator construction, mechanism, repairs, and reinstallations. SSRN Electron J [Internet]. 2023; Available from: http://dx.doi.org/10.2139/ssrn.4392601.

16. Wang W, Yang H, Chen Y, Huang X, Cao J, Zhang W. Motion analysis of wire rope maintenance device. Actuators [Internet]. 2023;12(10):392. Available from: http://dx.doi.org/10.3390/act12100392.

17. Babu Seelam A, Jawed MS, Hassan Krishanmurthy S. Design and analysis of elevator wire ropes. Int J Simul Multidiscip Des Optim [Internet]. 2021;12:20. Available from: http://dx.doi.org/10.1051/smdo/2021021.

18. Chen Y, Wang Q, Qin W, Xiang J. Study on the mechanical performance of a three-layered wire rope strand with a surface pit in varied corrosion direction into the wire. Eng Fail Anal [Internet]. 2022;136(106181):106181. Available from: http://dx.doi.org/10.1016/j.engfailanal.|2022.106181.

19. Youssef B, Meknassi M, Achraf W, Gugouch F, Lasfar S, Kane CSE, et al. The analysis of the corrosion effect on the wires of a 19*7 wire rope by two methods. Eng Fail Anal [Internet]. 2023;144(106816):106816. Available from: http://dx.doi.org/10.1016/j.engfailanal.2022.106816.

20. Peng Y, Wang G, Zhu Z, Chang X, Lu H, Tang W, et al. Effect of low temperature on tribological characteristics and wear mechanism of wire rope. Tribol Int [Internet]. 2021;164(107231):107231. Available from: http://dx.doi.org/10.1016/j.triboint.2021.107231.

21. Hu Z, Wang E, Jia F. Study on bending fatigue failure behaviors of end-fixed wire ropes. Eng Fail Anal [Internet]. 2022;135(106172):106172. Available from: http://dx.doi.org/10.1016/j.engfailanal.2022.106172.

22. Chang X, Peng Y, Zhu Z, Lu H, Tang W, Zhang X. Sliding friction and wear characteristics of wire rope contact with sheave under long-distance transmission conditions. Materials (Basel) [Internet]. 2022;15(20):7092. Available from: http://dx.doi.org/10.3390/ma15207092.

23. Peng Y, Huang K, Ma C, Zhu Z, Chang X, Lu H, et al. Friction and wear of multiple steel wires in a wire rope. Friction [Internet]. 2023;11(5):763-84. Available from: http://dx.doi.org/10.1007/s40544-022-0665-y.

24. Vordos N, Gkika D, Bandekas D. Wheatstone Bridge and Bioengineering. J Eng Sci Technol Rev [Internet]. 2020;13(5):4-6. Available from: http://dx.doi.org/10.25103/jestr.135.02.

25. General Purpose Rope 8×S (19)+ FC 8×W(19) + FC [Internet]. TAYMAX. [cited 2024 Sep 23]. Available from: http://www.taymax.co.th/product/general-purpose-rope-8xs-19-fc-8xw19-fc/?lang=th.

DOI: 10.60101/jarst.2024.260813

26. Oluwole OO, Olanipekun AT, Ajide OO. Design, construction and testing of a strain gauge instrument. International Journal of Scientific & Engineering Research. 2015;6(4):1825-9.

27. Zhao D, Gao C, Zhou Z, Liu S, Chen B, Gao J. Fatigue life prediction of the wire rope based on grey theory under small sample condition. Eng Fail Anal [Internet]. 2020;107(104237): 104237. Available from: http://dx.doi.org/10.1016/j.engfailanal.2019.104237.

28. Zhao D, Liu YX, Ren XT, Gao JZ, Liu SG, Dong LQ, et al. Fatigue life prediction of wire rope based on grey particle filter method under small sample condition. Eksploat Niezawodn - Maint Reliab [Internet]. 2021;23(3):454-67. Available from: http://dx.doi.org/10.17531/ein.2021.3.6.

29. Lotfy HM, El-Shabasy AB, Attia TA, Hassan HA. Assessment of steel wire's fatigue life using finite elements modelling and experimental testing. IOP Conf Ser Mater Sci Eng [Internet]. 2020;973(1):012013. Available from: http://dx.doi.org/10.1088/1757-899x/973/1/012013.

30. Battini D, Solazzi L, Lezzi AM, Clerici F, Donzella G. Prediction of steel wire rope fatigue life based on thermal measurements. Int J Mech Sci [Internet]. 2020;182(105761):105761. Available from: http://dx.doi.org/10.1016/j.ijmecsci.2020.105761.

31. Ding P, Yang Q, Wang C, Wei X, Zhou Y. Application of improved grey model GM(1,1) in prediction of human health data. In: 2018 IEEE Third International Conference on Data Science in Cyberspace (DSC). IEEE; 2018.

32. Yang H, Gao M, Xiao Q. A novel fractional-order accumulation GMP(1,1) model and its application [Internet]. Research Square. 2022. Available from: http://dx.doi.org/10.21203/rs.3.rs-201981/v1.

33. Yılmaz O, İmrak CE. Discard fatigue life of stranded steel wire rope subjected to bending over sheave fatigue. Mech Ind [Internet]. 2017; 18(2):223. Available from: https://doi.org/10.1051/meca/2016049.

34. Wang D, Wang B, Ge S, Wu K, Chong H, Zhang D, et al. Effects of fatigue load characteristics on bending tribo-corrosion-fatigue damage of steel wire ropes in seawater and pure water. Tribol Int [Internet]. 2025;201(110201):110201. Available from: http://dx.doi.org/10.1016/j.triboint.2024.110201.

35. Li C, Wang D, Sun Y, Xu W, Zhang J, Wu K, et al. Bending fatigue damage behavior of wire rope in hoisting system of drilling rig. Tribol Int [Internet]. 2023;187(108745):108745. Available from: http://dx.doi.org/10.1016/j.triboint.2023.108745.

36. Huang K, Peng Y, Chang X, Zhou Z, Jiang G, Lu H, et al. Fretting fatigue behavior of helical-torsional contact steel wire in wire rope. Int J Fatigue [Internet]. 2024;186(108393):108393. Available from: http://dx.doi.org/10.1016/j.ijfatigue.2024.108393.

37. Yang H, Gao M, Xiao Q. A novel fractional-order accumulation GMP(1,1) model and its application [Internet]. Research Square. 2022; Available from: http://dx.doi.org/10.21203/rs.3.rs-201981/v1.

38. Wang H, Zheng H, Tian J, He H, Ji Z, He X. Research on quantitative identification method for wire rope wire breakage damage signals based on multi-decomposition information fusion. Journal of Safety and Sustainability [Internet]. 2024;1(2):89-97. Available from: http://dx.doi.org/10.1016/j.jsasus.2024.02.001.

39. Wang D, Wang B, Ge S, Wu K, Chong H, Zhang D, et al. Effects of fatigue load characteristics on bending tribo-corrosion-fatigue damage of steel wire ropes in seawater and pure water. Tribol Int [Internet]. 2025;201(110201):110201. Available from: http://dx.doi.org/10.1016/j.triboint.2024.110201.

40. Ministerial regulation prescribing standards for the management and operations concerning safety, Occupational Health, and Working Environment related to Machinery, Cranes, and Boilers, B.E. 2564 (2021). (2021, August 6). Royal Gazette; Volume 138 (Part 52 A), p. 3-29.

41. The British Standards. Safety rules for the construction and installation of lifts - Part 1: Electric Lifts [Internet]. 2009. Available from: https://nobelcert.com/DataFiles/FreeUpload/EN%2081-22-2014.pdf.

42. Japanese Industrial Standard. Inspection standard of elevator, escalator and dumbwaiter JIS A 4302-1992 [Internet]. 1992. Available from: https://www.stdlink.com/standards/jis-a-4302-1992.html.

43. The British Standards. Safety rules for the construction and installation of lifts - Lifts for the transport of persons and goods Part 20: Passenger and goods passenger lifts [Internet]. 2014. Available from:https://nobelcert.com/DataFiles/FreeUpload/EN%2081-20-2014.pdf.

DOI: 10.60101/jarst.2024.260813